Journal of Oncology Research and Therapy
Goyal N, et al. Oncol Res Ther 8: 10172.
www.doi.org/10.29011/2574-710X.10172
www.gavinpublishers.com

OPEN ACCESS

GAVIN PUBLISHERS

Research Article

Study of Ceramide-Flavone Analogs Showing Self-Fluorescence and Anti-Proliferation Activities

Navneet Goyal[1*], Camilla Do[1], Miriam Hill-Odom[1], Teresa Beamon[1], Tulasi Ponnapakkam[1], Jiawang Liu[2], Jayalakshmi Sridhar[1], Thomas Huckaba[3], and Maryam Foroozesh[1]

[1]Department of Chemistry, Xavier University of Louisiana, New Orleans, LA, USA

[2]University of Tennessee Health Sciences Center, Memphis, TN, USA

[3]Department of Biology, Xavier University of Louisiana, New Orleans, LA, USA

[*]**Corresponding author:** Navneet Goyal, Department of Chemistry, Xavier University of Louisiana, New Orleans, LA, USA

Citation: Goyal N, Do C, Hill-Odom M, Beamon T, Ponnapakkam T, et al. (2023) Study of Ceramide-Flavone Analogs Showing Self-Fluorescence and Anti-Proliferation Activities. J Oncol Res Ther 8: 10172. DOI: 10.29011/2574-710X.10172

Received Date: 09 May, 2023; **Accepted Date:** 24 May, 2023; **Published Date:** 27 May, 2023

Abstract

Background: Many current anti-cancer drugs used to treat breast cancer mediate tumor cell death through the induction of apoptosis. Cancer cells, however, often acquire multidrug-resistance following prolonged exposure to chemotherapeutics. Consequently, molecular pathways involved in tumor cell proliferation have become potential targets for pharmacological intervention. Ceramides are tumor suppressor lipids naturally found in the cell membrane, and are central molecules in the sphingolipid signalling pathway.

Methods: Our lab has targeted the ceramide signaling pathway for potential pharmacological intervention in the treatment of breast cancer. Previously, we have shown that certain ceramide analogs have therapeutic potential in the treatment of chemo-sensitive and multidrug-resistant breast cancers. Using the most active analog from our previous studies as the lead compound, new analogs containing a flavone moiety were designed and synthesized. In general, flavone derivatives often show interesting pharmacological properties, and compounds based on these molecules have been found useful in many different therapeutic areas including anti-tumor, anti-coagulants, and anti-HIV therapy.

Results: Synthesis and biological evaluation of five new flavonoid ceramide analogs are reported here. These compounds were also shown to be self-fluorescent, which can be useful when investigating their distribution and action in cancer cells.

Conclusion: Four out of the five flavone ceramide analogs in this study showed significant anti-proliferation activities in the three cell lines studied, MDA-MB-232, MCF-7, and MCF-7TN-R; some showing varying degrees of selectivity. The mechanisms involved in cell proliferation inhibition are complicated and further studies are needed.

Keywords: Breast Cancer; Ceramides; Flavones; Fluorescence

Introduction

Accounting for 12.5% of new cancer cases annually, breast cancer is the most common cancer world-wide [1]. Each year over 250,000 women and over 2,500 men in the United States are diagnosed with breast cancer [1,2]. Breast cancer risks and outcomes are not the same for all, and are highly linked to genetics and environmental causes, as well as health disparities [2]. Although Caucasian women in the US have a higher diagnosis rate for breast cancer, African Americans and other minorities suffer from lower survival rates than Caucasians, partly due to their lower rates of clinical breast cancer screening including mammography and access to cutting-edge treatments [2]. The World Health Organization (WHO) also reports breast cancer death inequities across the world, with high-income countries showing high survival rates (about 90%) and low-income countries such as South Africa showing low survival rates (about 40%) [3].

Even though chemotherapy continues to be the most common method of treatment for breast cancers, after prolonged exposure to chemotherapeutic drugs, cancer cells often develop multidrug-resistance, making treatment more difficult [2,4]. Developing more effective and less systemically toxic treatments targeting drug-resistant breast cancers is thus of outmost importance.

Due to the crucial role of ceramides in cell death regulation, hundreds of anti-cancer ceramide analogs have been synthesized and investigated in recent years [4,5]. Ceramide analogs can be designed to target drug-resistant as well as drug-sensitive breast cancer cells [5-10]. Our previous work and that of many other research groups have shown that certain ceramide analogs preferentially inhibit the growth of chemo-resistant cancer cells in comparison to regular cancer cells [11-13].

In this study, the carbon chain length and functional groups of the backbone in the target compounds were kept the same as our previously reported analogs, to maintain optimal lipid solubility and facility of passage through membranes [11-15]. The main structural variation was the introduction of a flavone moiety on the carbonyl of the side-chain amide functional group. Since certain flavone derivatives have been shown to have anti-cancer properties [16,17], we hypothesized that introducing a flavone moiety into the ceramide structure will impact its interactions with ceramide downstream targets, and potentially inhibit cell proliferation. In our initial studies, these flavonoid ceramide analogs were found to be self-fluorescent. This property can be used to follow the molecules' movements and actions in the cells *in vitro* and further *in-vivo* [18,19]. Previously a number of fluorescent ceramide analogs were synthesized containing an additional fluorescent moiety or dye attachment [18-20]; however, this is the first time to our knowledge that the ceramide analog itself has been designed to have self-fluorescence properties.

The five target ceramide analogs reported here are structural isomers, and any differences observed in their activities should be due to the orientation of the flavone moiety leading to variations in shape and intermolecular interactions with the surrounding environment. Additional information regarding one of the five analogs was reported previously [6].

Materials and Methods

Syntheses

All flavone alcohol starting material were purchased from Indofine Chemical Company (Hillsborough, PA). The coupling reagents, bases, and solvents were purchased from Sigma-Aldrich (St. Louis, MO).

Compound **4** is used as a precursor for the syntheses of target ceramide analogs. We have optimized the conditions to perform its synthesis on a 10 g scale [15] (Figure 1). Compound **1**, an acid with a boc-protected amine group (1.0 eq), was treated with DCC (N,N'-dicyclohexylcarbodiimide, 1.1 eq), HOBt (1-hydroxyl benzotriazole, 1.1 eq), N-methyl morpholine (3.0 eq), and amine **2** (1.1 eq). Dichloromethane (DCM) was used as the solvent. The crude product was purified by recrystallization using ethyl acetate: hexane (2:1) to get the amide **3** (84% yield). Compound **3** was dissolved in DCM and treated with TFA (trifluoroacetic acid) to perform boc-deprotection to get compound **4**, which was purified by recrystallization using ethyl acetate [18].

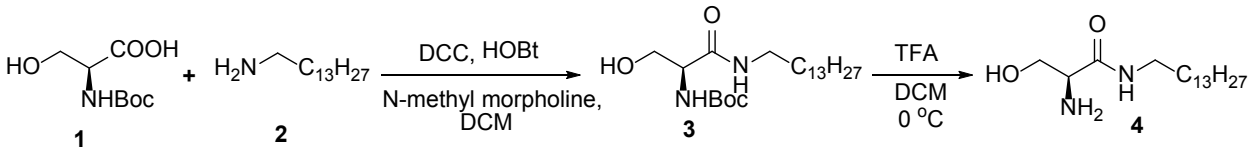

Figure 1: Synthesis scheme for compound 4.

Flavone-acids were synthesized using commercially available flavone alcohols or phenols as shown in Figure 2. The flavone alcohol or phenol **5** was dissolved in acetone in the presence of potassium carbonate (base) and reacted with bromoethyl acetate to get the corresponding ester intermediate **6**. Compound **6** was purified by column chromatography before hydrolyzation with potassium hydroxide (base) in methanol to get the corresponding carboxylic acid, compound **7**.

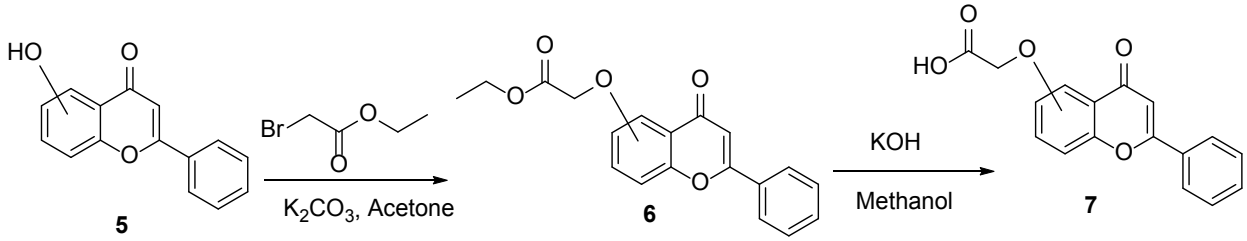

Figure 2: Synthesis scheme for the intermediate esters and acids.

The acid intermediate **7** was coupled with compound **4** using the coupling reagents EDCI (1-ethyl-3-(3-dimethylaminopropyl) carbodiimide) and HOBt in the presence of DIPEA (N,N- diisopropylethylamine) as a base and DCM as the solvent (Figure 3). The final flavone ceramide analog **8** was purified using Combiflash chromatography (hexane : ethyl acetate as the solvent).

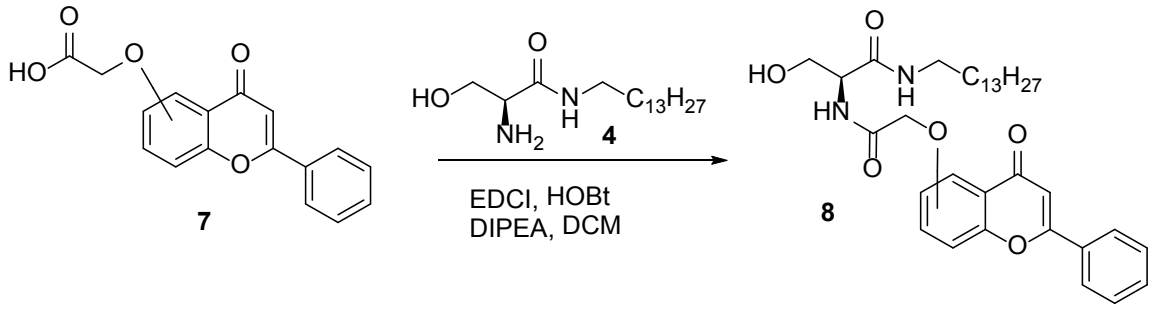

Figure 3. Last synthesis step leading to the final products.

The target compounds (Figure 4) were successfully synthesized with yields ranging from 10-71%. Since very small amounts of each of the analogs were needed for these studies, even the lower reaction yields were acceptable.

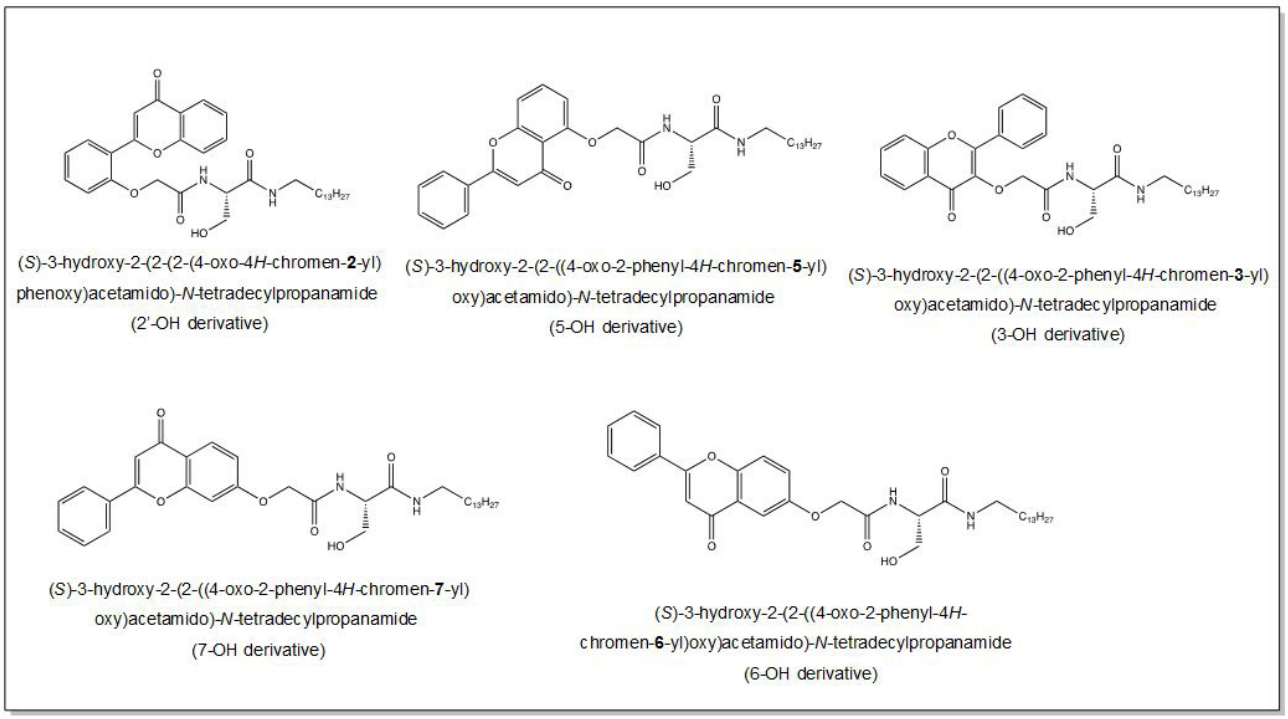

Figure 4: Structures of the target ceramide analogs, and the percent yield of each synthesis.

Bioassays

- **Cell lines:** *In vitro* studies were performed on the estrogen receptor (ER) positive chemo-sensitive MCF-7 breast cancer cell line (American Type Culture Collection (ATCC); catalog number HTB-22), as well as two drug-resistant breast cancer model systems, MDA-MB-231 (ATCC; catalog number HTB-26) and MCF-7TN-R. MDA-MB-231 cells are highly metastatic and triple-negative, lacking estrogen receptor (ER) and progesterone receptor (PR) expression, as well as human epidermal growth factor receptor 2 (HER2) amplification. MCF-7TN-R is a chemo-resistant breast cancer cell line derived from the chemo-sensitive breast cancer cell line MCF-7. MCF-7 cells were treated with the tumor necrosis factor alpha (TNF-α) until they acquired resistance to TNF-α-induced cell death. MCF-7TN-R cells are highly aggressive, and are also triple (ER/PR/Her2) negative. MCF-7TN-R cells used in this study were a gift from the Tulane University Medical Center.

Here, we studied the anti-cancer properties of the synthesized analogs, focusing on cell proliferation across these three cell lines.

- **Cell Culture**: MDA-MB-231, MCF-7,and MCF-7TN-R cells were cultured in Dulbecco's Modified Eagle Medium (DMEM) (Invitrogen; catalog number 11995-065) enriched with 10% fetal bovine serum (Gibco; catalog number 10437-028) and 1% antibiotic (antibiotic and antimycotic; Gibco; catalog number 15240-062). Cells were cultured in 75cm^2 tissue culture flasks in 37^{o}C humidified atmosphere of 5% CO_2 and 95% air.
- MTT Assays: MTT (3-(4,5-dimethylthiazol-2-yl)-2,5-diphenyltetrazolium bromide) colorimetric assays were performed on the newly synthesized compounds according to the manufacturer protocol (Life Technologies; catalog number M6494) to assess cell proliferation based on cell metabolic activity. Cells from each cell line were plated on 96-well plates at 15,000 cells/well in 200 µL of DMEM media in triplicates. Cells were incubated and given 24 hours to adhere to plates before removing the media. Cells were then treated with gradient concentrations of ceramide analogs in DMEM, or with dimethyl sulfoxide (DMSO) in DMEM as control, and incubated for an additional 48-hour period to allow proliferation. 20 µL of the MTT reagent was added to each well, followed by incubation for 2 hours. Media was carefully aspirated, and 150 µL of DMSO was added to dissolve the crystals. The absorbance of the plate was read using a Biotek Synergy H1 Microplate Reader at 550 nm.

Statistical Analyses: Graph Pad Prism software (Graph-Pad Software, Inc.) was used for calculating the IC_{50} values.

Docking Studies

Increased intracellular ceramide levels have been shown to increase apoptotic activity. Exogenous ceramides can be designed to cause inhibition of ceramide-metabolizing enzymes, such as ceramidase, leading to increased intercellular ceramide levels and apoptosis [21]. Ceramidase metabolizes ceramides into sphingosine, and is considered a regulator of cellular autophagy and drug-resistance in cancer cells [21]. To study the interactions of the five flavone ceramide analogs with the enzyme ceramidase in order to determine whether their anti-proliferation activities are due to the inhibition of this enzyme, their 3D structures were built using Molecular Operating Environment (MOE) from ChemComp Group. The X-ray crystal structure of ceramidase was obtained from the Protein Data Bank (2ZXC.pdb). Initial geometric optimizations of the ligands were carried out using the standard MMFF94 force field, with a 0.001 kcal/mol energy gradient convergence criterion and a distance-dependent dielectric constant employing Gasteiger and Marsili charges. Additional geometric optimizations were performed using the semi-empirical method molecular orbital package (MOPAC). Docking was performed using 'dock' module of the MOE software. The best docking pose was determined with visual inspection, considering the docking scores. Figure 5 shows the binding modes of the five analogs in the active site of the enzyme ceramidase. Figure 6 depicts the ligand interactions between our lead compound from previous studies, (S,E)-3-hydroxy-2-(2-hydroxybenzylidene)-amino-N-tetradecylpropanamide (analog 315) [15], and the flavone ceramide analogs with the ceramidase amino acid residues.

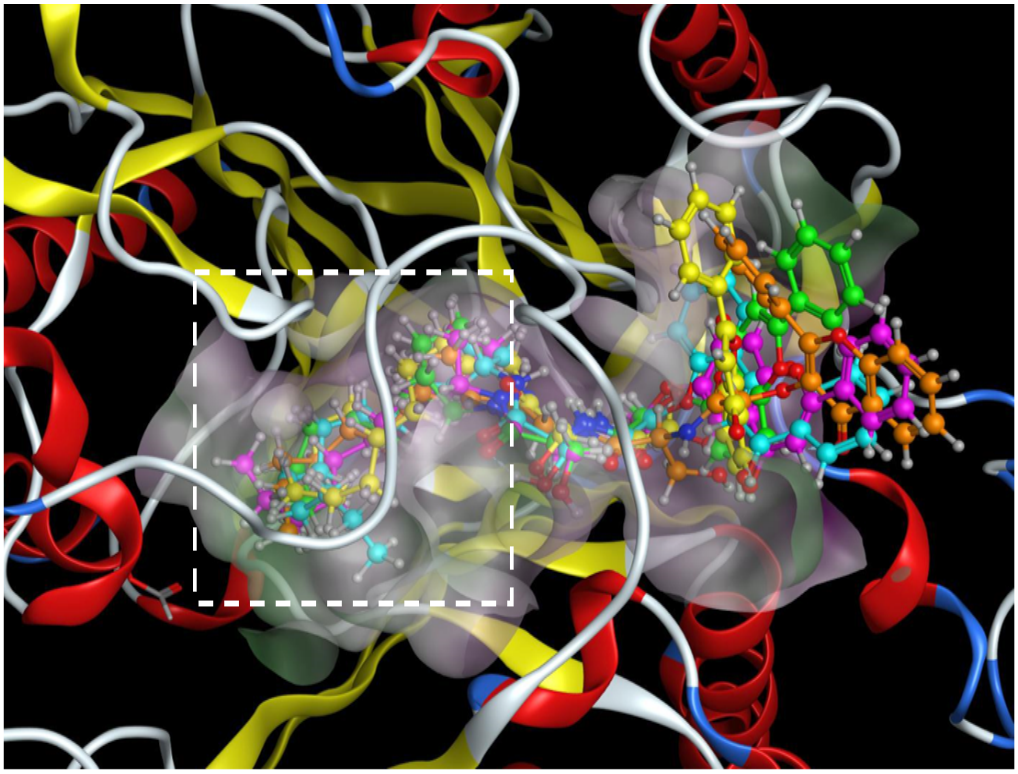

Figure 5: The binding modes of the flavone ceramide analogs derived from the 2'-OH (cyan), 3-OH (orange), 5-OH (green), 6-OH (pink) and 7-OH (yellow) flavones in the active site of the ceramidase protein X-ray crystal structure (2ZXC.pdb). The deep end of the pocket is outlined in the white box. The protein is shown as a ribbon model colored by secondary structure. The five analogs are shown as ball and stick models.

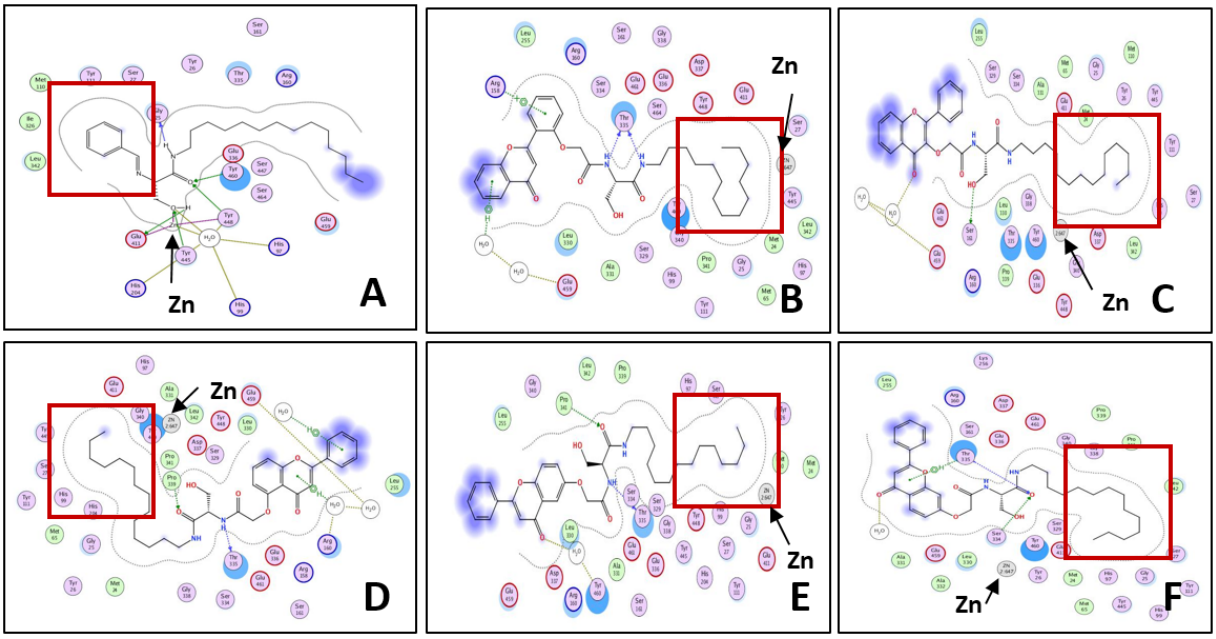

Figure 6: The ligand interaction pictures of (A) lead ceramide analog from previous studies (analog 315) and the flavone ceramide analogs derived from (B) 2'-OH, (C) 3-OH, (D) 5-OH, (E) 6-OH, and (F) 7-OH flavones. The deep end of the binding pocket is outlined by the red box.

Fluorescence Determination

MCF-7 cells were plated on glass bottom MatTek dishes at a concentration of 200,000 cells per dish and allowed to incubate for 24 hours. Compounds or vehicle (DMSO) were then added to the media in separate dishes at a final concentration of 50 µM, and allowed to incubate for four hours. Cellular uptake of compounds was then visualized via fluorescence microscopy using a Nikon A1 microscope. Fluorescence excitation occurred using an EXFO LED array with intensity fixed at 50% and filtered through a Nikon DAPI filter cube (375/28 ex, 460/60 em). Images were acquired through a Nikon PlanAPO 60x (1.40 NA) oil objective via an Andor EMCCD camera. All imaging was carried out with identical settings of a 400 millisecond acquisition and the gain set to zero on the EMCCD camera. To analyze the fluorescence intensity in each cell, raw images were opened in ImageJ, a line was drawn around each cell, and the mean gray value inside each cell was measured by the software. Data reported are the arithmetic mean of the mean gray value of at least 125 separate cells.

Results

Bioassays

In MTT assays, four out of the five synthesized compounds have shown anti-proliferative activity against the breast cancer cell lines used (Figure 7). Data is shown in Table 1. The analog derived from 2'-OH flavone showed IC_{50} values of 12.56, 12.52, and 24.59 µM in MDA-MB-231, MCF-7 and MCF-7TN-R cell lines, respectively, showing selectivity towards the first two. The compound derived from 3-OH flavone showed IC_{50} values of 10.67, 19.33 and 14.56 µM in MDA-MB-231, MCF-7, and MCF-7TN-R cell lines, respectively, showing some selectivity towards MDA-MB-231. The analog derived from 5-OH flavone showed the lowest levels of anti-proliferative activity in all three cell lines. The analog derived from 6-OH flavone showed IC_{50} values of 13.76, 13.72, and 13.17 µM for MDA-MB-231, MCF-7, and MCF-7TN-R cell lines, respectively, showing no selectivity. The molecule derived from 7-OH flavone showed IC_{50} values of 18.38, 18.39, and 24.24 µM in MDA-MB-231, MCF-7 and MCF-7TN-R cell lines, respectively, showing better activity in MDA-MB-231 and MCF-7 cell lines (Figure 7).

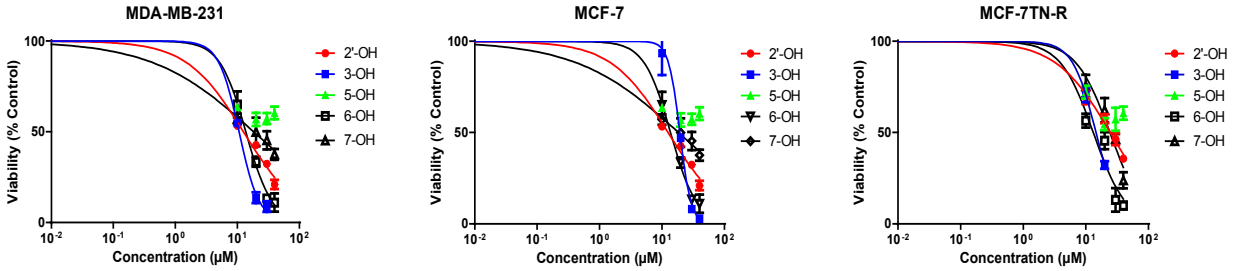

Figure 7: MTT assay results in the three cell lines studied.

Analog/Cell Line	MDA-MB-231	MCF-7	MCF-7TN-R
2'- OH	12.56 +/-0.32	12.52 +/-0.23	24.59 +/-0.44
3-OH	10.67 +/-0.09	19.33 +/-0.52	14.56 +/-0.87
5-OH	75.07 +/-18.47	86.57 +/-2.68	43.78 +/-7.94
6-OH	13.76 +/-0.72	13.72 +/-0.42	13.17+/-0.53
7-OH	18.38 +/-0.21	18.39 +/-0.16	24.24+/-0.67

Table 1: IC_{50} values (μM) +/- SE for the five new analogs in the three breast cancer cell lines studied.

Measuring anti-proliferative effects has provided the basis for large scale screenings of cytotoxic drugs. Anti-proliferative assays measure growth inhibition rather than cell death. Results of our experiments clearly indicates that four out of the five analogs show anti-proliferative effects. This class of compounds are potential candidates for new drug treatment, and further studies are needed to elucidate the mechanisms of action.

Analog derived form 2-OH flavone shows significant selectivity in its strong anti-proliferative effects on MDA-MB-231 and MCF-7 cells compared to MCF-7TN-R cells. For the analog derived from 3-OH flavone, MTT assays show the lowest IC_{50} value for MDA-MB-231 cells, followed by MCF-7TN-R, and the highest for MCF-7 cells. Results for the analog derived from 5-OH flavone shows no significant anti-proliferative activity in any of the cell lines. The results for the analog derived from 6-OH flavone shows strong anti-proliferative activity in all three cell lines with no selectivity. The results observed for the analog derived from 7-OH shows the lowest anti-proliferative activity in the MCF-7TN-R cells.

Docking Studies

All flavone ceramides docked with the hydrophobic aliphatic backbone chain extending deep inside of the binding pocket of ceramidase. Depending on the position of attachment of the flavone moiety to the ceramide backbone, the flavone ring system made hydrogen bonds to different amino acid residues on the periphery of the binding cavity. For the ceramide analogs derived from 3-OH and 6-OH flavones, the carbonyl of the flavone ring system made hydrogen bonds with the water molecule that bridged a network of hydrogen bonds from the ligand to the protein residue Glu459. The ceramide analog derived from 6-OH flavone made a similar hydrogen bonding network with bridging water molecule to the residue Tyr460. The backbone amide carbonyls of 5-OH, 6-OH and 7-OH flavone derived molecules made hydrogen bonds to the residues Pro339, Pro341 and Ser334, respectively. One or both amide NH groups of 2'-OH, 5-OH and 6-OH flavone derived molecules formed hydrogen bonds with Thr335. The backbone hydroxyl group of the analog derived from 3-OH flavone was the only one to form a hydrogen bond with the residue Ser161. Aromatic-hydrogen interactions were also seen between the flavone rings of 2'-OH, 5-OH, and 7-OH flavone derived analogs with the residues Glu459, Arg160, and Thr335, respectively. Overall, of the five analogs, the analog derived from 6-OH flavone showed the most number of hydrogen bonding interactions with the binding pocket amino acid residues either directly or through a bridge water molecule (Glu459, Tyr460, Pro341, and Thr335).

The orientation of the flavone ceramides docked in the active site of the enzyme ceramidase were opposite to that observed for the ceramide analog 315 molecule (Figure 8). The phenyl ring of the ceramide analog 315 resided in the deep end of the binding cavity whereas for the flavone ceramides, the long hydrophobic backbone chain resided in the same space. This flipping of the

binding orientation of the flavone ceramides resulted in concomitant changes to the orientation of the rest of the molecule with the flavone ring system extending on the periphery of the entry way of the access channel to the active site. The degree of extension of the hydrophobic chain into the binding cavity and the variations in the positioning of the flavone moiety on the periphery of the active site binding cavity resulted in differences in the positioning of the centrally located backbone amide and hydroxymethyl functional groups in the long passage cavity that forms a channel to the active site Zn atom. These functional groups in all five flavone ceramides were kept far from the Zn atom, while in ceramide analog 315 were in close proximity to this atom. These subtle changes also resulted in differences in hydrogen bonding pattern for these centrally located functional groups with the protein amino acid residues. These changes in the binding poses of the flavone ceramides resulted in the loss of some key interactions with the ceramidase active site, which could have resulted in the reduced inhibition potency for these compounds compared to analog 315.

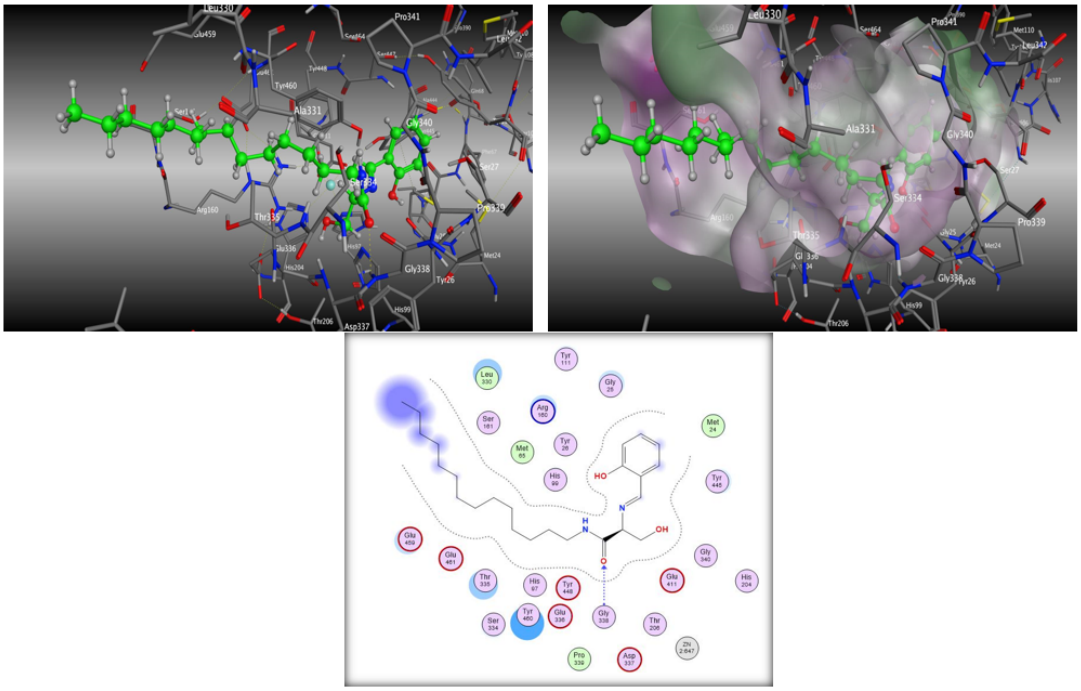

(8A) Binding mode 1: The carbonyl of the analog 315 forms a hydrogen bond to the backbone NH of the residue Gly338. The entire molecule fits well into the binding cavity.

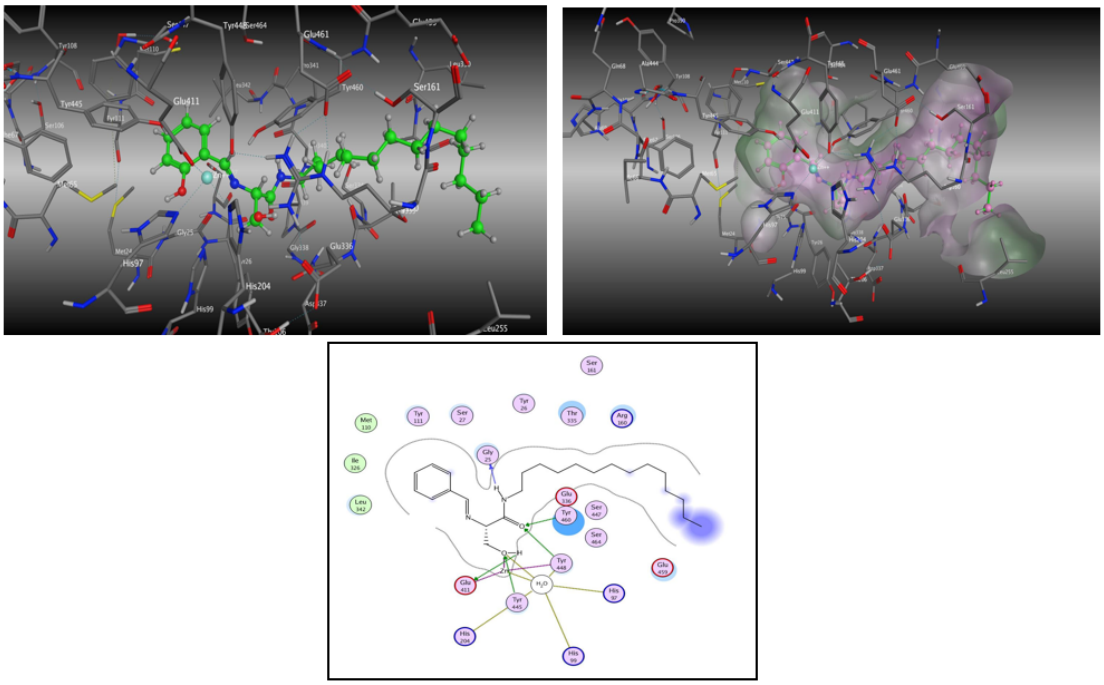

(8B) Binding mode 2: The benzene ring resides deep inside the pocket in close proximity to the zinc atom. There is no hydrogen bonding with the binding site residues. However, the molecule fits well in the cavity.

Figure 8. Binding modes for analog 315.

Fluorescence Studies

Representative images for 2'-OH and 3-OH flavone analogs, and vehicle are shown in Figure 9. Images in the top row have been auto contrasted in Image to visualize cells. Note the background haze in the images of 2'-OH and vehicle indicative of high contrast and narrow brightness ranges necessary to see any fluorescent signal in the cells. Images in the bottom row have been set to the brightness and contrast settings of the 3-OH auto-contrasted image, resulting in comparably equivalent fluorescence intensity across all three images. While the fluorescence signal of cells incubated with 2'-OH flavone ceramide was no greater than vehicle, there was a significant increase in fluorescence intensity in cells incubated with 3-OH flavone ceramide.

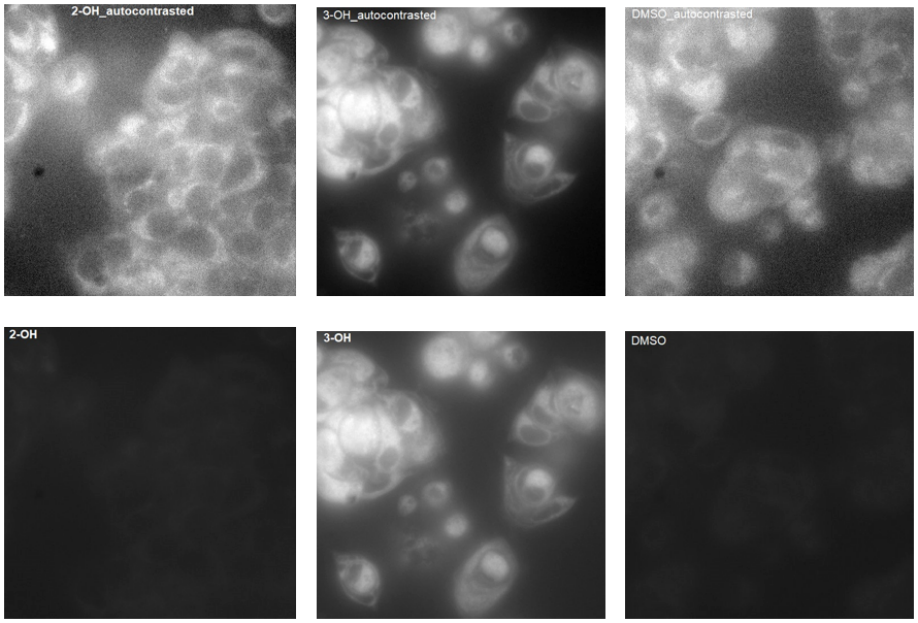

Figure 9: 2'-OH flavone ceramide, 3-OH flavone ceramide, and vehicle treated MCF-7 cells.

Bar graph in Figure 10 shows the average mean gray value inside each cell (i.e. fluorescence intensity captured by the EMCCD over the pixels corresponding to each cell) in a series of images. Data shown is for >125 cells for each. Error bars show the standard deviation.

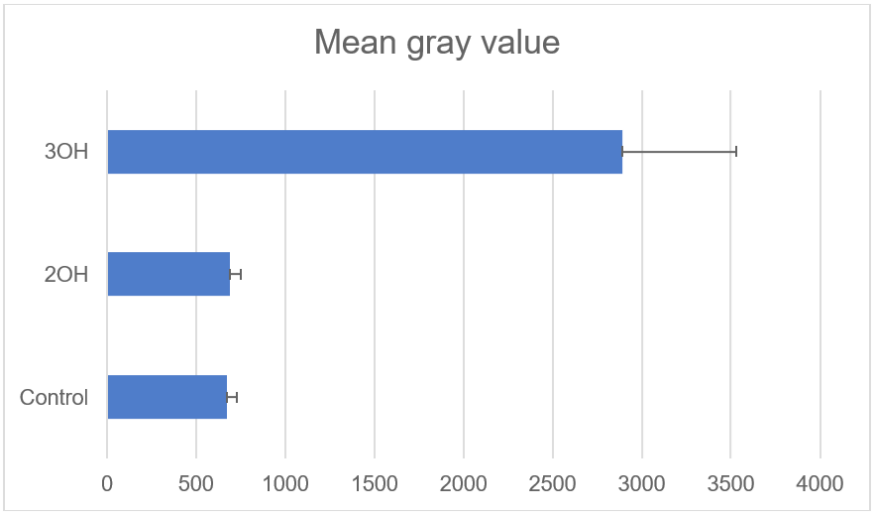

Figure 10: Mean gray value 2'-OH flavone ceramide, 3-OH flavone ceramide, and vehicle treated MCF-7 cells.

Conclusions

We successfully synthesized a new series of five ceramide analogs in which a flavone moiety was introduced on the side-chain amide functional group. These compounds showed varying degrees of self-fluorescence and anti-proliferative activity in MCF-7, MCF-7TN-R, or MDA-MB-231 cell lines. Four out of the five compounds showed significant anti-proliferation activities in the three cell lines, with some showing different degrees of selectivity.

Based on the results of the docking studies with the enzyme ceramidase, the flavone moiety seems to be too large to fit into the binding cavity. The flipped orientation of the analogs in the binding pocket oriented the hydroxypropanamide part of the structures in the channel of the binding pocket away from the Zn atom resulting in decreased inhibition potency, thus, the anti-proliferation activities observed here are not due to the inhibition of this enzyme. Our lead compound, analog 315, has a much smaller benzene ring moiety and shows higher degree of interactions with this enzyme's active site (Figure 8). The mechanisms of action of the flavonoid ceramide analogs seem to be different from those of analog 315, at least in relation to ceramidase inhibition.

Acknowledgement

Research reported in this publication was supported by the National Institute of General Medical Sciences of the National Institutes of Health under Award Number 5RL5GM118966, National Cancer Institute of the National Institutes of Health AREA grant 1R15CA159059, the NIMHD-RCMI grant number 5G12MD007595, and the Louisiana Cancer Research Center. The content is solely the responsibility of the authors and does not necessarily represent the official views of the National Institutes of Health or the Louisiana Cancer Research Center.

References

1. Understanding Breast Cancer.
2. American Cancer Society. Cancer Facts & Figures (2022).
3. The Global Breast Cancer Initiative. Breast Cancer Inequities.
4. Morad SAF, Cabot MC (2013) Ceramide-Orchestrated Signaling in Cancer Cells. Nature Reviews Cancer 13: 51-65.
5. Liu J, Beckman BS, Foroozesh M (2013) A Review of Ceramide Analogs as Potential Anticancer Agents. Future Med Chem 5: 1405-1421.
6. Dai L, Goyal N, Lin Z, Valle LD, Chen J, Zabaleta J, Liu J, Foroozesh M, Qin Z (2020) Developing New Ceramide Analogs and Identifying Novel Sphingolipid Controlled Genes Against a Virus-Associated Lymphoma. Blood E-ISSN:1528-0020.
7. Simstein R, Burow M, Parker A, Weldon C, Beckman B (2003) Apoptosis, Chemoresistance, and Breast Cancer: Insights from the MCF-7 Cell Model System. Exp. Biol. Med. 228, 995-1003.
8. Shabbits JA, Mayer LD (2002) P-Glycoprotein Modulates Ceramide Mediated Sensitivity of Human Breast Cancer Cells to Tubulin-Binding Anticancer Drugs. Mol. Cancer Ther. 1: 205-213.
9. Gouaze-Andersson V, Yu JY, Kreitenberg AJ, Bielawska A, Giuliano AE, Cabot MC (2007) Ceramide and Glucosylceramide Upregulate Expression of the Multidrug Resistance Gene MDR1 in Cancer Cells. Biochim. Biophys. Acta 1771 (12): 1407-1417.
10. Liu YY et al (2008) A Role for Ceramide in Driving Cancer Cell Resistance to Doxorubicin. FASEB J. 22, 2541-2551.
11. Antoon JW, Liu J, Gestaut MM, Burow ME, Beckman BS, Foroozesh M (2009) Design, Synthesis, and Biological Activity of a Family of Novel Ceramide Analogues in Chemoresistant Breast Cancer Cells. J Med. Chem. 52(18): 5748-5752.
12. Liu J, Antoon W, Ponnapakkam A, Beckman B.S, Foroozesh M (2010) Novel Anti-Viability Ceramide Analogs: Design, Synthesis, and Structure-Activity Relationship Studies of Substituted (S)-2-(benzylideneamino)-3-hydroxy-N-tetradecylpropanamides. Bioorg. Med. Chem. 18(14): 5316-5322.
13. Ponnapakkam T, Saulsberry T, Hill T, Hill-Odom M, Goyal N, Anbalagan M, Foroozesh M (2018) Inhibition of Breast Tumor Growth in Mice After Treatment With Ceramide Analog 315. Anticancer Drugs 29(9): 898-903.
14. Goyal N, Do C, Donahue JP, Mague JT, Foroozesh M (2018) Ethyl 2-[2-(4-oxo-4H-chromen-2-yl)phenoxy]-acetate. IUCrData 3: x180993.
15. Foroozesh M, Goyal N, Jackson T, Do C, Booker S, Hill T, Liu J (2017) Optimization of Scale-up Synthesis of Anti-cancer Ceramide Analog 315. Journal of Undergraduate Chemistry Research 12: 89-91.
16. Wong ILK et al (2021) Flavonoid Monomer as Potent, Nontoxic, and Selective Modulators of the Breast Cancer Resistance Protein (ABCG2). J. Med. Chem. 64(19): 14311-14331.
17. Goyal N, Liu J, Lovings L, Dupart P, Taylor S, Bellow S, Mensah L, McClain E, Dotson B, Sridhar J, Zhang X, Zhao M, Foroozesh M (2014) Ethynylflavones, Highly Potent and Selective Inhibitor of Cytochrome P450 1A1. Chem. Res. Toxicol 27: 1431-1439.
18. Pagano RE, Martin OC, Kang HC, Haugland RP (1991) A Novel Fluorescent Ceramide Analogue for Studying Membrane Traffic in Animal Cells: Accumulation at the Golgi Apparatus Results in Altered Spectral Properties of the Sphingolipid Precursor. J. Cell Biol.113: 1267-1279.
19. Pagano RE, Sleight RG (1985) Defining Lipid Transport Pathways in Animal Cells. Science 229:1051-1057.
20. Matsufuji T, Kinoshita M, Matsumori N (2019) Preparation and Membrane Distribution of Fluorescent Derivatives of Ceramides. Langmuir 35: 2392-2398.
21. Gomez-Larrauri A, Das AU, Aramburu-Nuñez M, Custodia A, Ouro A (2021) Ceramide Metabolism Enzymes—Therapeutic Targets Against Cancer. Medicina 57: 729.

Study of Ceramide-Flavone Analogs Showing Self-Fluorescence and Anti-Proliferation Activities (Structural analysis data)

(S)-3-hydroxy-2-(2-(2-(4-oxo-4H-chromen-2-yl)phenoxy)acetamido)-N-tetradecylpropanamide: (2'-OH analog): (71%, grey solid); GC-MS showed m/z: 578.75, 300.0, 279.0; ^{1}HNMR ($CDCl_3$, 300 MHz) δ = 8.23-8.39 (m, 2H), 8.05-8.15 (m, 3H), 7.75-7.86 (m, 2H), 7.36-7.69 (m, 2H), 4.64-4.78 (m, 1H), 4.85 (s, 2H), 3.83-3.90 (m, 1H), 3.30-3.40 (m, 2H), 1.57-1.68 (m, 4H), 1.16-1.38 (m, 24H), 0.90 (t, *J* = 6..7 Hz, 3H); ^{13}C NMR ($CDCl_3$, 75 MHz) δ = 178.5, 172.4, 169.0, 162.5, 158.0, 157.5, 132.5, 128.5, 127.4, 126.0, 122.1, 118.0, 117.5, 110.0, 72.5, 71.0, 69.0, 38.0, 32.0, 29.4, 29.2, 29.0, 28.5, 22.7, 14.5.

(*S*)-3-hydroxy-2-(2-((4-oxo-2-phenyl-4*H*-chromen-3-yl)oxy)acetamido)-*N*-tetradecylpropanamide: (3-OH analog)

(40%, white solid); GC-MS showed m/z: 578.75, 300.0, 279.0; ^{1}HNMR ($CDCl_3$, 300 MHz) δ = 8.10-8.25 (m, 1H), 7.70-8.15 (m, 6 H), 7.36-7.69 (m, 2H), 4.90 (s, 1H), 4.85 (s, 2H), 4.35-4.50 (m, 2H), 3.83-3.90 (m, 1H), 3.30-3.50 (m, 2H), 1.16-1.67 (m, 24 H), 0.90 (t, *J* = 6..7 Hz, 3H); ^{13}C NMR ($CDCl_3$, 75 MHz) δ = 179.5, 174.4, 171.0, 160.5, 159.0, 158.5, 132.5, 128.5, 128.4, 126.0, 121.0, 118.0, 110.0, 74.5, 72.0, 69.0, 38.0, 33.0, 29.7, 29.5, 29.0, 28.5, 22.7, 14.0.

(*S*)-3-hydroxy-2-(2-((4-oxo-2-phenyl-4*H*-chromen-5-yl)oxy)acetamido)-*N*-tetradecylpropanamide: (5-OH analog) (49%, white solid): GC-MS showed m/z: 578.75, 300.0, 279.0; ^{1}HNMR ($CDCl_3$, 300 MHz) δ = 8.00-8.10 (m, 1H), 7.50-8.15 (m, 7 H), 6.70 (s, 1H), 4.83 (s, 2H), 4.30-4.45 (m, 2H), 3.80-3.85 (m, 1H), 3.20-3.10 (m, 2H), 1.10-1.60 (m, 24 H), 0.85 (t, *J* = 6..7 Hz, 3H); ^{13}C NMR ($CDCl_3$, 75 MHz) δ = 177.5, 168.4, 167.0, 161.5, 132.5, 128.5, 128.4, 127.4, 126.5, 126.0, 121.0, 117.0, 112.0, 76.5, 71.0, 69.5, 38.5, 33.5, 29.8, 29.2, 28.5, 23.5, 14.5.

(*S*)-3-hydroxy-2-(2-((4-oxo-2-phenyl-4*H*-chromen-6-yl)oxy)acetamido)-*N*-tetradecylpropanamide: **(6-OH analog)** (10%, white solid): GC-MS showed m/z: 578.75, 300.0, 279.0; ^{1}HNMR ($CDCl_3$, 300 MHz) δ = 8.10 (s, 1 H), 7.90-8.05 (m, 8H), 7.75-7.86 (m, 2H), 7.36-7.69 (m, 2H), 4.64-4.78 (m, 1H), 4.85 (s, 2H), 3.83-3.90 (m, 1H), 3.30-3.40 (m, 2H), 1.57-1.68 (m, 4H), 1.16-1.38 (m, 24H), 0.90 (t, *J* = 6..8 Hz, 3H); ^{13}C NMR ($CDCl_3$, 75 MHz) δ = 185.2, 181.0, 175.0, 172.0, 165.5, 157.5, 132.0, 129.3, 127.5, 127.0, 126.7, 126.5, 126.0, 122.1, 118.1, 72.5, 69.0, 38.5, 32.0, 29.4, 29.2, 29.0, 28.0, 22.5, 14.2.

(*S*)-3-hydroxy-2-(2-((4-oxo-2-phenyl-4*H*-chromen-7-yl)oxy)acetamido)-*N*-tetradecylpropanamide: **(7-OH analog)**: (21%, white solid): GC-MS showed m/z: 578.75, 300.0, 279.0; ^{1}HNMR ($CDCl_3$, 300 MHz) δ = 8.05-8.10 (m, 1H), 7.65-7.90 (m, 7H), 6.90 (s, 1H), 4.65 (s, 1H), 4.80 (s, 2H), 3.83-3.95 (m, 1H), 3.30-3.35 (m, 2H), 1.16-1.55 (m, 28H), 0.92 (t, *J* = 6..8 Hz, 3H); ^{13}C NMR ($CDCl_3$, 75 MHz) δ = 177.5, 171.4, 169.5, 167.0, 166.2, 162.5, 157.0, 156.2, 132.0, 128.0, 127.8, 126.5, 122.0, 117.2, 110.6, 71.5, 69.5, 38.0, 32.0, 29.5, 29.4, 29.2, 28.7, 22.9, 14.0.